VIBRATION OF MULTI-STAGE GEAR DRIVES INFLUENCED BY NONLINEAR COUPLINGS

Miroslav Byrtus
Department of Mechanics
Faculty of Applied Sciences
University of West Bohemia
Czech Republic
byrtus@kme.zcu.cz

Vladimír Zeman
Department of Mechanics
Faculty of Applied Sciences
University of West Bohemia
Czech Republic
zemanv@kme.zcu.cz

Abstract

This paper deals with mathematical modelling of nonlinear vibration of multi-stage large rotating shaft systems with gears and rolling-element bearings. Gearing and bearing couplings bring into the system nonlinear phenomena like impact motions due to the possibility of the mesh interruption. The motion of the system is then influenced by the internal kinematic excitation in gearing, by the parametric excitation caused by periodic change of number of teeth in gear meshing and can be further influenced by impacts of freely rotating gears which transmit no static torque. The developed methodology is tested for gear drive vibration of a two-stage gearbox.

Key words

Gear drives, vibration, modal synthesis method, nonlinear systems, bifurcation, chaos.

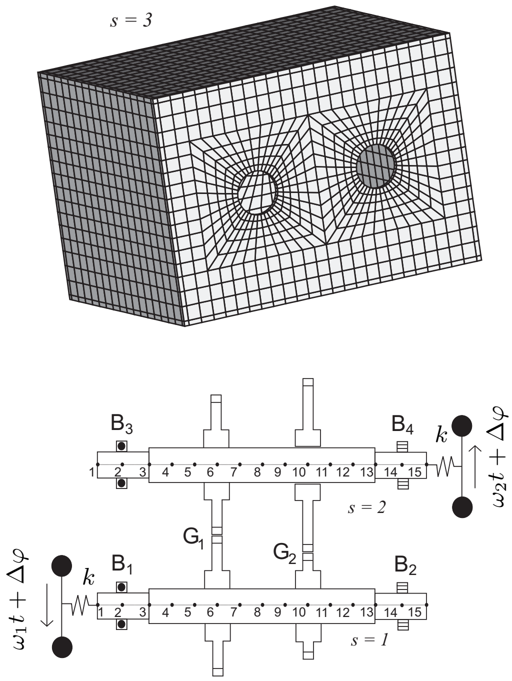

Figure 1. Scheme of two-stage gearbox.

1 Introduction

Large rotating systems, especially gear drives and gearboxes occur as parts of many mechanical devices transmitting the torque with relatively small loss of power. But they represent main internal excitation sources of these systems. Their vibration analyses are commonly performed with the assumption of the small deformations and linearized coupling forces. But this assumption is not correct for certain operational states when the influence of coupling nonlinearities is dominant. Therefore, the nonlinear models of gear and bearing couplings are developed and the influence of coupling nonlinearities is investigated. In last years the subject of large rotating system modelling has been studied in our department. The result of this effort is a creation of modal synthesis method allowing to model systems with complicated structures. The advantage of this method is the separated modelling of subsystems using different modelling tools and separated modelling of discrete couplings. Each coupling is described by geometrical and material properties and by corresponding coupling force characteristics. The main contribution of the modal synthesis method consists in the degrees of freedom number (DOF) reduction, which is based on the transformation described by a transformation matrix assembled from chosen eigenmode shapes of subsystems. The selection of suitable eigenmode shapes is mostly governed by the range of exciting force frequency spectrum. The final condensed mathematical model has then significantly lower number of DOF than the original mathematical model and can be advantageously used for numerical investigation of nonlinear effects caused by nonlinear coupling characteristics or by parametric excitation in couplings. This contribution is focused on modelling of a model gearbox vibration (figure 1) which is supposed to be included into a drive between two wheels by means of discrete torsional couplings characterized by torsional stiffnesses k. The driving and driven wheels rotate by the constant angular speeds ω_1 and ω_2 and the static loading of rotating parts of the gearbox is defined by the initial static torsional drive deformation $\Delta\varphi$ between wheels. The gearbox vibrations are excited by kinematic transmission errors of gear pairs transmitting the power and by their time dependent meshing stiffnesses.

2 Modelling of gearboxes

Presented approach to the gearbox modelling uses the modal synthesis method based on suitable system decomposition into subsystems and on separate modelling of couplings among subsystems.

2.1 Modelling of subsystems

Generally, the subsystems rotating with angular velocity ω_s are described in local generalized coordinates $\mathbf{q}_s(t)$ with system of n_s ordinary differential equations in matrix form [Zeman and Hlavac, 1995]

$$\begin{aligned} &\mathbf{M}_s\ddot{\mathbf{q}}_s(t) + (\mathbf{B}_s + \omega_s\mathbf{G}_s)\dot{\mathbf{q}}_s(t) + \mathbf{K}_s\mathbf{q}_s(t) = \\ &= \mathbf{f}_s^E(t) + \mathbf{f}_s^B + \mathbf{f}_s^G, \qquad\qquad s = 1, 2, \ldots, S, \end{aligned} \tag{1}$$

where $\mathbf{M}_s$, $\mathbf{B}_s$ and $\mathbf{K}_s$ are symmetrical mass, damping and stiffness matrices of the uncoupled subsystems of order n_s and $\mathbf{G}_s$ is skew symmetrical matrix of the gyroscopic effects of the same order for $s = 1, 2, \ldots, S-1$ only. These matrices are usually created by means of finite element method combined with discrete parameters representing masses of rigid gear discs. External forced excitation is described by vector $\mathbf{f}_s^E(t)$. Vector $\mathbf{f}_s^B$ expresses the coupling forces in rolling-element bearings and vector $\mathbf{f}_s^G$ represents the forces in spur helical gear couplings. All force effects described in vectors above are acting on the subsystem s.

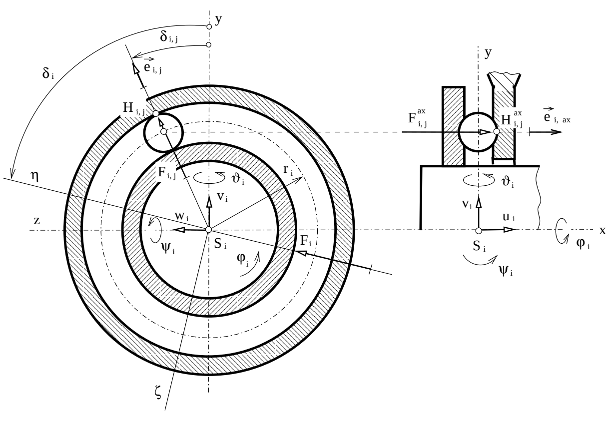

Figure 2. Scheme of a bearing coupling

2.2 Bearing model

The bearing model, used here, respects real number of rolling elements uniformly distributed between the inner and outer race (see figure 2).

Then the vector $\mathbf{f}_s^B$ in equation (1) (model of rotating parts) can be expressed in following form [Byrtus and Zeman, 2005]

$$\mathbf{f}_s^B = -\sum_{i,j}(\tilde{\boldsymbol{t}}_{i,j}F_{i,j} + \tilde{\boldsymbol{t}}_{i,j}^{ax}F_{i,j}^{ax}), \tag{2}$$

where vectors $\tilde{\boldsymbol{t}}_{i,j}$, $\tilde{\boldsymbol{t}}_{i,j}^{ax}$ describe the bearing geometry. Among bearing indices i belong only these which correspond to bearings coupled with the subsystem s, $s = 1, \ldots, S-1$. Similarly, the vector $\mathbf{f}_S^B$ in equation (1) (model of a stator – housing) can be expressed in following form

$$\mathbf{f}_S^B = \sum_{i,j}(\tilde{\boldsymbol{e}}_{i,j}F_{i,j} + \tilde{\boldsymbol{e}}_{i,j}^{ax}F_{i,j}^{ax}), \tag{3}$$

where vectors $\tilde{e}_{i,j}$, $\tilde{e}_{i,j}^{ax}$ describe the geometry of contact points at the stator. Bearing indices i are governed by the same conditions as above.

In the general coordinate space

$$\mathbf{q} = [\,\mathbf{q}_1^T,\ \mathbf{q}_2^T,\ \ldots\ ,\ \mathbf{q}_S^T\,]^T \in \mathbb{R}^n, \quad n = \sum_{s=1}^{S} n_s \tag{4}$$

of the whole system the bearing model is described by the global coupling vector in the form

$$\mathbf{f}^B = \begin{bmatrix} \mathbf{f}_1^B \\ \mathbf{f}_2^B \\ \vdots \\ \mathbf{f}_S^B \end{bmatrix} = \sum_{i,j}(\mathbf{c}_{i,j}F_{i,j} + \mathbf{c}_{i,j}^{ax}F_{i,j}^{ax}). \tag{5}$$

Vectors $\mathbf{c}_{i,j}$ and $\mathbf{c}_{i,j}^{ax}$ describe global geometrical properties of each bearing contact point j in bearing i and have this structure

$$\begin{aligned} \mathbf{c}_{i,j} &= \left[\,\cdots\ -\tilde{\mathbf{t}}_{i,j}^T \cdots\ \tilde{\mathbf{e}}_{i,j}^T\ \cdots\right]^T, \\ \mathbf{c}_{i,j}^{ax} &= \left[\,\cdots\ -(\tilde{\mathbf{t}}_{i,j}^{ax})^T \cdots\ (\tilde{\mathbf{e}}_{i,j}^{ax})^T\ \cdots\right]^T. \end{aligned} \tag{6}$$

To stabilize the numerical simulation of the nonlinear model it is efficient to separate the linear part of nonlinear bearing force characteristic. The linear part is described by stiffness and damping matrices in the general coordinate space (4) and the bearing force vector (5) can be then rewritten in following form

$$\mathbf{f}^B = -\mathbf{K}_B\mathbf{q} - \mathbf{B}_B\dot{\mathbf{q}} + \sum_{i,j}(\mathbf{c}_{i,j}f_{i,j} + \mathbf{c}_{i,j}^{ax}f_{i,j}^{ax}), \tag{7}$$

where $\mathbf{K}_B$ and $\mathbf{B}_B$ are global stiffness and damping bearing matrices. Their structure depends on the number of rolling elements and on the nodal points to which they are fixed on the shafts (for details see [Zeman and Hajzman, 2005]). The bearing damping matrix is supposed to be proportional to the stiffness matrix

$$\mathbf{B}_B = \beta_B\mathbf{K}_B \tag{8}$$

and functions $f_{i,j}(\Delta_{i,j})$ and $f_{i,j}^{ax}(\Delta_{i,j}^{ax})$ respect the possibility of contact loss between the rolling-element j and the outer race in the bearing i and depend on linearized rolling-elements stiffness that is calculated in dependence on an external static torsional load of driving and driven shafts [Byrtus and Zeman, 2005].

2.3 Gearing model

The force effect of the spur helical gear coupling G_z (figure 1) in (1) is expressed by vector

$$\mathbf{f}_s^G = \pm \sum_z \tilde{\boldsymbol{\delta}}_{z,i} F_z(t, d_z, \dot{d}_z), \tag{9}$$

where sign ”-” (minus) corresponds to driving gear and sign ”+” (plus) corresponds to driven gear (figure 3). Vector $\tilde{\boldsymbol{\delta}}_{z,i} = [\ldots, \boldsymbol{\delta}_{z,i}^T, \ldots]^T$ is the n_s-dimensional extended vector given by geometrical parameters α (normal pressure angle), β (angle of inclination of the teeth), γ (angle of position vector), r_i (rolling radius of the gear). The driving (driven) gear is fixed on the shaft at the nodal point i (j). Details are shown in [Zeman and Hlavac, 1995]. The resultant force F_z transmitted by gearing z can be approximately expressed in the form

$$F_z(t, d_z, \dot{d}_z) = k_z(t) d_z + b_z \dot{d}_z + f_z(t, d_z), \tag{10}$$

where $k_z(t)$ is time dependent meshing stiffness and b_z is coefficient of viscous damping of gearing on gear mesh line. Nonlinear function $f_z(t, d_z)$ of gearing deformation d_z corrects the linear elastic part of the force F_z in the phases of the gear mesh interruption.

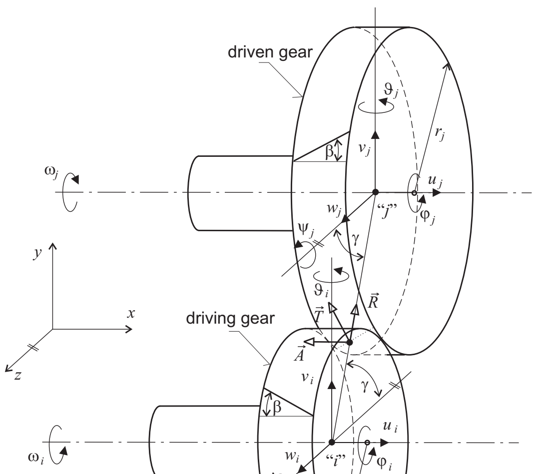

Figure 3. Scheme of a gearing coupling

Gearing deformation

$$d_z(t) = -\boldsymbol{\delta}_{z,i}^T \mathbf{q}_i(t) + \boldsymbol{\delta}_{z,j} \mathbf{q}_j(t) + \Delta_z(t) \tag{11}$$

of gears in mesh fixed on shafts at nodal points i and j expresses the relative motion of theoretical contact point of teeth on the gear mesh line. Vectors $\mathbf{q}_i(t) = [\ldots u_i\, v_i\, w_i\, \varphi_i\, \vartheta_i\, \psi_i\, \ldots]^T$ and $\mathbf{q}_j(t)$ having similar form describe displacements of nodal points i and j. The function $\Delta_z(t)$, defining kinematic transmission error of gearing z, can be expressed by Fourier series

$$\Delta_z(t) = \sum_{k=1}^{K} (\Delta_{z,k}^C \cos k\omega_z t + \Delta_{z,k}^S \sin k\omega_z t), \tag{12}$$

where ω_z are meshing frequencies.

Analogous to the bearing model, we can express the global gear coupling vector in general coordinate space (4) in following way

$$\mathbf{f}^G = \begin{bmatrix} \mathbf{f}_1^G \\ \mathbf{f}_2^G \\ \vdots \\ \mathbf{f}_{S-1}^G \\ \mathbf{0} \end{bmatrix} = \sum_{z=1}^{Z} \mathbf{c}_z F_z(t, \mathbf{q}, \dot{\mathbf{q}}) + \mathbf{f}_G(t), \tag{13}$$

where $\mathbf{f}_G(t)$ is vector of internal kinematic excitation generated in gear meshing that can be expressed in form

$$\mathbf{f}_G(t) = \sum_{z=1}^{Z} \Big(k_z(t) \Delta_z(t) + b_z \dot{\Delta}_z(t) \Big) \mathbf{c}_z. \tag{14}$$

The global vector of geometrical parameters of the gearing z in general coordinate space (4) has following structure

$$\mathbf{c}_z = \left[\cdots - \boldsymbol{\delta}_{z,i}^T \cdots \boldsymbol{\delta}_{z,j}^T \cdots \middle| \mathbf{0}^T \right]^T. \tag{15}$$

For the same reason as above, it is efficient to separate up the linear part of nonlinear gearing force characteristic. Equation (13) can be then rewritten to this form

$$\mathbf{f}^G = -\mathbf{K}_G \mathbf{q} - \mathbf{B}_G \dot{\mathbf{q}} + \sum_{z=1}^{Z} \mathbf{c}_z f_z(t, \mathbf{q}) + \mathbf{f}_G(t), \tag{16}$$

where $\mathbf{K}_G$ and $\mathbf{B}_G$ are global linearized stiffness and damping matrices of gear couplings whose structure is described in detail in [Zeman and Hajzman, 2005].

2.4 Parametric excitation in gear coupling

The behaviour of the gearing is moreover influenced by the periodic time-varying meshing stiffness whose mathematical model has come through a longtime progress. In the first contributions published in the fifties the meshing stiffness was considered to be constant equal to the mean meshing stiffness. Because of the change of tooth pair stiffness during the mesh, different gearing models were developed. The stiffness of a particular tooth pair is considered to be periodic. The period depends on the duration of one tooth pair mesh. It is influenced by the tooth profile, profile error, gear contact ratio and lubricant properties in gearing.

Particular courses of the mesh stiffness can be expressed in a analytical way. Authors [Cai and Hayashi, 1994] proposed the gear mesh stiffness $k_p(t)$ for a tooth pair p in the form

$$\begin{aligned} k_p(t) &= k_m K_p(t) \quad \text{for} \quad t \in \langle t_p, t_p + \varepsilon_\gamma T \rangle, \\ k_p(t) &= 0 \qquad\qquad\quad \text{otherwise} \end{aligned} \tag{17}$$

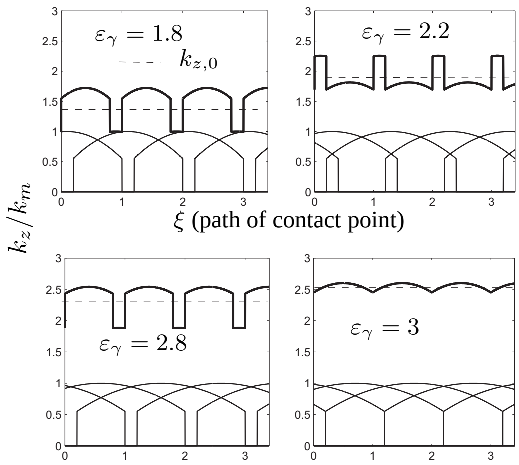

Figure 4. Relative gear mesh stiffness for different values of contact ratio ε_γ.

where

$$K_p(t) = \left(\frac{-1.8}{(\varepsilon_\gamma T)^2}(t-t_p)^2 + \frac{1.8}{\varepsilon_\gamma T}(t-t_p) + 0.55 \right) \tag{18}$$

depending on the contact ratio ε_γ and on the period of the gear mesh. The parameter k_m represents maximal value of the gear mesh stiffness of one tooth pair on the assumption that at time $t = t_p$ teeth enter into mesh and at $t = t_p + \varepsilon_\gamma T$ get out of the mesh. The gear mesh period is then equal to $T = (2\pi)/(p_z\omega)$, where parameter p_z indicates the number of the teeth of the drive gear mounted on a shaft rotating with angular velocity ω.

Figure 4 shows the dependance of the relative meshing stiffness k_z/k_m on the path of the contact point in the front plane of the gearing for different values of contact ratio ε_γ. The parameter $k_{z,0}$ corresponds to the mean meshing stiffness. The bold lines display the resulting gear mesh stiffness, which is given as a sum of the stiffnesses of teeth being in the gear mesh for a given time. The resulting meshing stiffness can be expressed in following form

$$k_z(t) = \sum_p k_p(t), \tag{19}$$

where index p is restricted to the tooth pairs being in gear mesh for the given time t.

2.5 Condensed mathematical model

It is advantageous to assemble condensed mathematical model of the system with reduced degrees of freedom (DOF) number, because, in particular, the housing subsystem could have too large DOF number and this can hinder from consecutive performing of various dynamical analyses. The modal transformations

$$\mathbf{q}_s(t) = {}^m\mathbf{V}_s \mathbf{x}_s(t), \qquad s = 1, 2, \dots, S, \tag{20}$$

are introduced for this purpose. Matrices ${}^m\mathbf{V}_s \in \mathbb{R}^{n_s, m_s}$ are modal submatrices obtained from modal analysis of the mutually uncoupled, undamped and non-rotating subsystems, whereas m_s ($m_s \leq n_s$) is the number of the chosen master modes of vibration. The new configuration space of the dimension m is defined by vector

$$\mathbf{x} = [\, \mathbf{x}_1^T,\, \mathbf{x}_2^T,\, \dots,\, \mathbf{x}_S^T \,]^T, \qquad m = \sum_{s=1}^{S} m_s. \tag{21}$$

The model (1) can be then rewritten using terms (7) and (16) in the global condensed form

$$\begin{aligned}
&\ddot{\mathbf{x}}(t) + \Big(\mathbf{B} + \omega_0 \mathbf{G} + \mathbf{V}^T\left(\mathbf{B}_B + \mathbf{B}_G\right)\mathbf{V}\Big)\dot{\mathbf{x}}(t) + \\
&\quad + \Big(\boldsymbol{\Lambda} + \mathbf{V}^T\left(\mathbf{K}_B + \mathbf{K}_G\right)\mathbf{V}\Big)\mathbf{x}(t) = \\
&\quad = \mathbf{V}^T \Big(\sum_i \sum_j (\mathbf{c}_{i,j} f_{i,j}(\mathbf{q}) + \mathbf{c}_{i,j}^{ax} f_{i,j}^{ax}(\mathbf{q})) + \\
&\quad + \sum_{z=1}^{Z} \mathbf{c}_z f_z(t, \mathbf{q}) + \mathbf{f}_G(t) + \mathbf{f}_E(t) \Big),
\end{aligned} \tag{22}$$

where $\mathbf{f}_E(t) = [\, (\mathbf{f}_1^E(t))^T,\, (\mathbf{f}_2^E(t))^T,\, \dots,\, (\mathbf{f}_S^E(t))^T \,]^T$ is the global vector of external excitation,

$$\begin{aligned}
\mathbf{B} &= \mathrm{diag}\left({}^m\mathbf{V}_s^T \mathbf{B}_s {}^m\mathbf{V}_s \right), \\
\mathbf{G} &= \mathrm{diag}\left(\frac{\omega_s}{\omega_0}\, {}^m\mathbf{V}_s^T \mathbf{G}_s {}^m\mathbf{V}_s \right), \\
\mathbf{V} &= \mathrm{diag}\left({}^m\mathbf{V}_s \right)
\end{aligned} \tag{23}$$

are block diagonal matrices ($\omega_S = 0$ holds for the stator subsystem) and $\boldsymbol{\Lambda} = \mathrm{diag}\left({}^m\boldsymbol{\Lambda}_s \right)$ is diagonal matrix assembled of spectral submatrices ${}^m\boldsymbol{\Lambda}_s \in \mathbb{R}^{m_s, m_s}$ of the subsystems.

3 Analysis of two-stage gearbox vibration

The mathematical model of gear drive is strongly nonlinear due to the possibility of gear mesh interruption and in consequence of nonlinear bearing couplings respecting loss of contact in some contact points in dependance on position of journal centre. To perform the dynamical analysis the condensed mathematical model (22) has to be transformed into the state space to use the time integration method. The time integration is started from the initial state

$$\begin{aligned}
\mathbf{x}(0) &= (\boldsymbol{\Lambda} + \mathbf{V}^T(\mathbf{K}_B + \mathbf{K}_G)\mathbf{V})^{-1}\mathbf{V}^T\mathbf{f}_E(0), \\
\dot{\mathbf{x}}(0) &= \boldsymbol{\omega}_0
\end{aligned} \tag{24}$$

to minimize the startup transient motions. Vector $\boldsymbol{\omega}_0$ expresses the initial angular speed of shafts. In general, the vector $\mathbf{f}_E(0)$ can describe an arbitrary external excitation at the start of numerical integration.

The presented methodology was applied to the two-stage gearbox (figure 1) which can be disassembled into three subsystems – drive shaft with gears ($s = 1$), driven shaft with gears ($s = 2$) and housing ($s = 3$) wired in selected nodal points with the fixed frame. Subsystems are joined by discrete couplings – gear meshings G_z ($z = 1, 2$) and rolling-element bearings (B_1 to B_4) considering twenty rolling-elements in each bearing. The initial number of DOF of the uncoupled subsystems after discretization by FEM using MATLAB code for rotating subsystems and software package ANSYS for housing was $n_1 = 90$ (drive shaft), $n_2 = 91$ (driven shaft) and $n_3 \sim 15000$ (housing). Numerical experiments show that the reduced (condensed) model (22) of the complete system of the order $m = 160$ ($m_1 = 30$, $m_2 = 30$, $m_3 = 100$) is acceptable in the frequency range up to 5000 Hz.

The gearbox vibration was investigated for the first transmission degree, when gearing G_1 transmits the power. The second gear pair rotates freely about the deformed shaft axles. The vibration is caused by the internal kinematic excitation in the form (14) for $z = 1$ and by the time-varying change of meshing stiffness $k_1(t)$ in the form (18) and (19). Only three first amplitudes of the Fourier series (12) were taken into account and have following values

$$\Delta^S_{1,1} = 5 \cdot 10^{-6}\,\mathrm{m}, \quad \Delta^S_{1,2} = \frac{\Delta^S_{1,1}}{2}, \\ \Delta^S_{1,3} = \frac{\Delta^S_{1,1}}{3}, \quad \Delta^C_{1,1} = \Delta^C_{1,2} = \Delta^C_{1,3} = 0. \tag{25}$$

3.1 Constant gear mesh

The linearized condensed model (22) for zero nonlinear functions ($f_{i,j}(\mathbf{q}) \equiv 0$, $f^{ax}_{i,j}(\mathbf{q}) \equiv 0$ and $f_z(t, \mathbf{q}) \equiv 0$) was used for determination of the constant gear mesh regions. Using the linearization we neglect the possibility of gear mesh interruption and we consider constant stiffness given by static loading of each rolling-element in all bearings. Supposing the internal kinematic excitation in gearing defined by (12), (14) and (25), we can investigate for which operational parameters – revolutions per minute and static load – the gear mesh is constant and we can find a boundary of interrupted gear mesh.

From knowledge of the time response of the system in configuration space $\mathbf{x}(t)$ we can formulate the condition of constant gear mesh z

$$\min_{t \in T} d_z(t) = \min_{t \in T} \{-\mathbf{c}_z^T \mathbf{V}\mathbf{x}(t) + \Delta_z(t)\} > 0. \tag{26}$$

This condition generally holds for both linearized and full nonlinear model of the gearbox.

Figure 5 shows area of interrupted gear mesh (white area) and of constant gear mesh (grey area) of the first gear mesh transmitting the power in dependence on two operational parameters – on revolutions per minute of the driving shaft and on external static preload acting on rotating disks mounted to drive and driven shafts. Results were gained from the linearized model for steady state motion. The steady gearing deformations are then expressed by Fourier series with above mentioned harmonic components with the fundamental frequency equal to the meshing frequency. There are

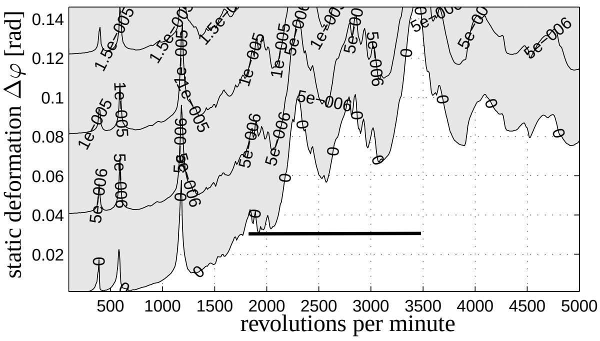

Figure 5. Map of constant gear mesh of first gearing G_1.

many peaks corresponding to resonance states of the gearbox on the boundary between constant and interrupted gear mesh. The gear box shows greater displacements and thence greater gearing deformations and greater tendency towards gear mesh interruption in all resonance states.

3.2 Nonlinear two-stage gearbox vibration

Further, we are concerned with the qualitative analysis of the two-stage gearbox nonlinear vibration, which is influenced by gear mesh interruption and time-varying meshing stiffness. The nonlinear model includes such nonlinear phenomena like impacts in gearing and nonlinear contact forces transmitted by rolling-elements of bearings. These phenomena, which are shown for systems with several DOF number in [Thomson, 2002], are sources of nonlinear effects in solution of the model. The time response of such a system is accompanied by bifurcation of solution in dependence on chosen operational parameters. Vibro-impact systems are characterized by period doubling scenario, when the period number of the time response increases unexpectedly twice for a certain values of operational parameters. This scenario could repeat till the motion becomes chaotic. Moreover, the time response of nonlinear model is influenced by impacts in gear meshings with one freely rotating gear. Here, we investigate the influence of the phase shift between the kinematic and parametric excitation in gearing G_1. All results introduced here are gained for the condensation level of the gearbox and for kinematic transmission errors mentioned in the chapter before.

Figure 6 shows bifurcation diagrams of gearing deformation of gearing G_1 for a chosen revolution range of the gearbox, which is inscribed with the bold black line in figure 5. The corresponding statical external preload is characterized by torsional doformation $\Delta\varphi = 0.03$ rad. In each bifurcation diagram a line designating the zero gearing deformation is plotted. Each dot plotted under this line corresponds to gear mesh interruption during one period of motion. Grey dots agree with local maxima of gearing deformation and the black ones agree with local minima, respectively. In the chosen operational area exist periodical solutions

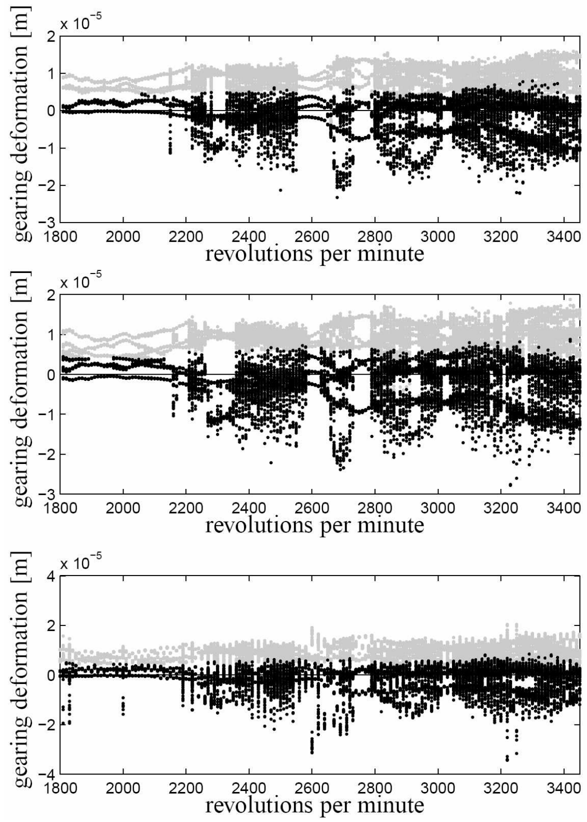

Figure 6. Bifurcation diagrams of the gearing deformation G_1.

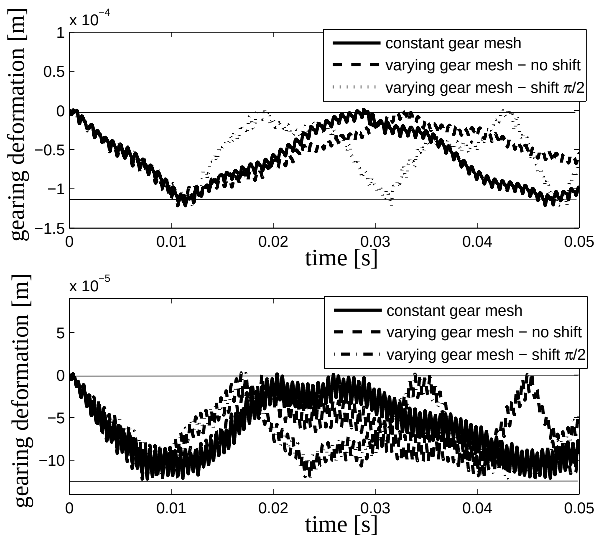

Figure 7. Gearing deformation of the freely rotating gear in gear mesh G_2.

which follow the period doubling scenario. This nonlinear phenomenon mostly accompanies the crossing of the area of constant gear mesh, as [Byrtus and Zeman, 2005] shows. Since the time course of the gearing deformation has a quasi-periodical structure, it is very difficult to detect points of period doubling in the diagram 6. The three diagrams showed here, correspond to constant meshing stiffness (above), time-varying meshing stiffness with no shift between the parametric and kinematic excitation (in the middle) and time-varying meshing stiffness with a phase shift equal to $\pi/2$ between the parametric and kinematic excitation (below).

Figure 7 shows gearing deformation in gear mesh G_2 with the freely rotating gear for the three above mentioned states and for 2000 rpm (above, characterized by periodical response) and 3000 rpm (below, characterized by chaotic response). The deformations are bounded by the gearing clearance showed by the two bold lines.

4 Conclusion

The paper describes the methodology of the large coupled rotating systems modelling and the analysis of their nonlinear vibrations. The models of these systems suppose a flexible shafts and stator and nonlinear gear couplings between rotor subsystems and nonlinear rolling-element bearings. The whole system model is created by means of the modal synthesis method which allows to reduce number of degrees of freedom of the mathematical model. The methodology is applied to the two-stage gearbox to simulate the dynamic response caused by kinematic transmission error of gears and by time-varying meshing stiffnesses. Vibration is accompanied by nonlinear phenomena like bifurcation, periodic and quasi-periodic solutions and chaos. These modes of motions are very interesting from the theoretical point of view and for gearbox design from the dynamic loading and noise point of view.

This work was supported by the research project MSM 4977751303 of the Ministry of Education, Youth and Sports of the Czech Republic and by the Research Project number 2A-2TP1/139 of Ministry of Industry and Trade of the Czech Republic.

References

Byrtus, M. and Zeman, V. (2005) Modelling and analyses of gear drive nonlinear vibration. In *Proc. of the Fifth EUROMECH Nonlinear Dynamics Conference*, Eindhoven, August 7-12, pp. 66-67 (full text on cd-rom).

Cai, Y. and Hayashi, T. (1994) The linear approximated equation of vibration of a pair of spur gears (Theory and experiment). In *Journal of Mechanical Design*, **116**, pp. 558-564.

Thompson, J. M. and Stewart, H. B. (2002) Nonlinear dynamics and chaos. John Wiley & Sons, Chichester.

Zeman, V. (1994) Dynamics of rotating machines by the modal synthesis method. In *Proceedings of the Tenth World Congress IFToMM*, Oulu, Finland, June 20 – 24, pp. 1668-1673.

Zeman, V. and Hajžman, M. (2005) Modelling of shaft system vibration with gears and rolling element bearings. In *Proc. of Colloquium Dynamics of Machines 2005*, Prague, February 8-9, pp. 163-170.

Zeman, V. and Hlaváč, Z. (1995) Mathematical modelling of vibration of gear transmissions by modal synthesis method. In *Proceedings of the Ninth World Congress on the Theory of Machines and Mechanisms*, Vol. 1, pp. 397-400, Politechnico di Milano, Italy.